Biophysical Journal Volume 70 April 1996 1872–1880

Myosin Head Orientation and Mobility During Isometric Contraction: Effects of Osmotic Compression

Bishow B. Adhikari and Piotr G. Fajer
Institute of Molecular Biophysics, National High Magnetic Field Laboratory and Department of Biological Science, Florida State University, Tallahassee, Florida 32306 USA

ABSTRACT We have correlated the mobility and the generation of force of myosin heads by applying radial compression to isometrically contracting muscle fibers. Osmotic pressure was produced by dextran T-500, and its effect on the orientation and mobility of myosin heads labeled with *N*-(1-oxy-2,2,5,5-tetramethyl-4-pyperidinyl)maleimide was observed by conventional and saturation-transfer electron paramagnetic resonance methods. A biphasic behavior in spectral changes coinciding with the tension dependence was observed as the fibers were compressed. At diameters above the equilibrium spacing, the large myosin head disorder characteristic during contraction in the absence of compression was largely maintained, whereas the mobility decreased threefold, from τ_R ~25 μs to ~80–90 μs. The inhibition of fast microsecond motions was not accompanied by tension loss, implying that these motions are not necessary for force generation. At diameters below the equilibrium spacing, both the disorder and the mobility decreased dramatically in parallel with the tension inhibition, suggesting that slower microsecond motions and the disorder of the myosin head are necessary for muscle function.

INTRODUCTION

According to the currently held theories of muscle contraction, the interaction of myosin heads with actin filaments involves a reorientation of the heads, while attached to the actin filaments (Huxley, 1969; Huxley and Simmons, 1971). The transition from one attached state to the next is thought to induce strain. If shortening is allowed, sliding of the two filaments relieves the strain; otherwise, tension is generated along the fiber axis. Detachment and subsequent reorientation then take the myosin heads back to their initial positions. Hydrolysis of ATP by myosin provides the chemical fuel for this cyclic process. Although challenged recently (Yanagida et al., 1985; Harada et al., 1987, 1990), the general assumption is that a one-to-one correspondence exists between the chemical states of the hydrolysis cycle and the structural states of the actomyosin complex (Lymn and Taylor, 1971; Eisenberg and Hill, 1985).

Because the interaction of myosin heads with actin filaments must involve a dynamic sequence of structural changes, characterization of the dynamics and orientational geometry of the interacting proteins is important. Previous electron paramagnetic resonance (EPR) studies have revealed a broad orientational distribution of myosin heads during isometric contraction at steady state (Cooke et al., 1982; Fajer et al., 1990b). Mobility of myosin heads during contraction, determined by saturation transfer electron paramagnetic resonance (ST-EPR) and phosphorescence, was found to be half that during relaxation (Barnett and Thomas, 1989; Stein et al., 1990). These observations in fibers and complementary studies of the acto-myosin subfragment 1 complexes in solution have led to the suggestion that both the broad orientations and the relatively uninhibited mobility of the myosin heads are important for force generation (Berger et al., 1989; Berger and Thomas, 1991, 1993), but a direct correlation between force and the myosin head distribution and mobility has never been demonstrated.

The difficulty of demonstrating a correlation between force and myosin-head dynamics and orientation lies in the spectral assignment in EPR of various populations of myosin heads existing during the steady-state hydrolysis. The perturbation of the force-generating myosin heads facilitates such an assignment and allows identification of orientations and dynamics important for the generation of force. In EPR studies, various methods of myosin head perturbation have been used in the past, most of which involved trapping one or a few well-defined states of the hydrolysis cycle by chemical analogs, such as AMPPNP, ATPγS, PP_i, BDM, ADP, and aluminum fluoride (Fajer et al., 1988; Fajer et al., 1995; Pate and Cooke, 1988; Zhao et al., 1995a; Fajer, 1994; Raucher and Fajer, 1994). An alternative approach is to use mechanical rather than biochemical cycle perturbation. The cross-bridges in any given state can be strained by either positive or negative forces along the fiber axis or by compression along the fiber radius. A number of studies showed that radial compression on isometrically contracting fibers leads to an inhibition of the axial force (Maughan and Godt, 1979; Gulati and Babu, 1982, 1985; Kawai et al., 1993). Radial compression is thought to perturb primarily the force-generating state and the state in which work is performed, the two slowest steps in the cycle where large-scale rearrangement of the myosin head is likely to occur (Zhao and Kawai, 1993), suggesting that such a perturbation might enable us to study specific force-generating transitions of the heads.

Received for publication 15 September 1995 and in final form 23 January 1996.

Address reprint requests to Dr. Piotr G. Fajer, National High Magnetic Field Laboratory, Florida State University, 1800 E. Paul Dirac Dr., Tallahassee, FL 32306-3016. Tel.: 904-644-2600; Fax: 904-644-1366; E-mail: fajer@sb.fsu.edu.

0006-3495/96/04/1872/09 $2.00

We report here changes in the orientations and mobility of myosin heads as a function of radial compression with varying concentrations of dextran T-500. Both the head orientations and dynamics exhibited a biphasic behavior that was closely correlated to the tension dependence. The two phases were separated by a critical lattice spacing. Compression up to the critical spacing resulted in small but significant changes in mobility and orientation without a loss of tension, whereas dramatic changes, accompanied by a sharp decline in tension, were observed at higher compression.

MATERIALS AND METHODS

Sample preparation

Skeletal muscle fibers were obtained from adult New Zealand white rabbits. Rabbits were killed by CO_2 asphyxiation, bled, and immediately cooled on ice. Strips of psoas (~4–6 mm in diameter) were removed, tied to acrylic sticks, and immersed in fiber-glycerinating buffer (FGB) (see Table 1 for solution composition) for 24 h while gently shaking to remove membrane from the muscle tissue. The fibers were then incubated in fiber storage buffer (FSB) for another 36 h and stored at −20°C for a maximum of 6 months. Unless stated otherwise, all preparative procedures were carried out at 4°C.

Spin labeling

We dissected fibers in FSB into thinner (~0.3–0.5 mm diameter) bundles and incubated them in 120 mM DTNB (5,5′-dithiobis[2-nitrobenzoic acid]) in rigor buffer (RB (KAc)) for 2 h before labeling, to preblock reactive SH sites not protected by the rigor cross-bridges (Zhao et al., 1995a). The fibers were then labeled by incubation in 0.25 mM MSL (*N*-[1-oxyl-2,2,2,6-tetramethyl-4-piperidinyl]maleimide; Aldrich Chemical Co., Milwaukee, WI) and 10 mM PP_i in RB (KAc) at pH 6.5 for 20 min. After labeling, the preblocked sites were reduced by incubation in 30 mM DTT (dithiothreitol) in RB (KAC) for 30 min at 23°C, washed several times in RB, and soaked in FSB for 30 min before storing at −20°C.

Typically 60–75% of the SH1 thiol groups of myosin were labeled by MSL, as estimated from the fractional inhibition of K/EDTA-ATPase (Crowder and Cooke, 1984). Labeling specificity was also determined by inspection of the rigor spectrum. The small peak in the low field region before the well-ordered three peaks of rigor spectrum (Fig. 3) accounts for ~10–15% of the total signal, as determined by spectral subtraction of relaxation spectrum from the rigor spectrum, indicating 85–90% spins are specific for SH-1. Physiological ATPases of labeled fibers were within 90% of unlabeled fibers. The average isometric tension of labeled fibers was 1.57 ± 0.08 kg/cm^2, which was 89% of unlabeled fibers (average tension = 1.76 ± 0.12 kg/cm^2).

ATPase assays

The ATPase activity was determined by measurement of the rate of inorganic phosphate release by myofibrils (~3–5 mg/ml) in the presence of saturating amounts of ATP. ATPase activity was measured under physiological and high-salt conditions, the latter for the determination of the amount of labeling. Protein concentration was determined by the biuret assay using bovine serum albumin (BSA) as a standard.

High-salt ATPase activity was measured at a myofibril concentration of ~3 mg/ml in 0.6 M KCl, 50 mM 3-(*N*-morpholino)propane-sulfonic acid (MOPS), at pH 7.5, and 10 mM EDTA for the K/EDTA-ATPase or 10 mM $CaCl_2$ for the Ca/K-ATPase. Physiological ATPase activity was measured in both relaxing solution (25 mM MOPS, 2 mM $MgCl_2$, 1 mM EGTA, pH 7.0) and contracting solution (relaxation plus 1.5 mM Ca^{2+}); both solutions were adjusted to 170 mM ionic strength with KPr, at a myofibril concentration of ~0.2–0.4 mg/ml. Both measurements were carried out at 25°C. The reaction was activated by adding either 5 mM ATP for high salt or 5 mM MgATP for the physiological ATPase activity. At timed intervals, the reacting myofibril solution was added to a fixed assay volume (1.6 ml) of MG-AM-ST (mixture of 0.045% malachite green, 34 mM ammonium molybdate in 4 N HCl and sterox in a 3:1:50 ratio) and quenched after 30 s with 34% citrate. The amount of the inorganic phosphate (P_i) in the assay tubes was determined by absorption at 660 nm.

Osmotic compression

Osmotic compression was achieved by the addition of dextran T-500 (Pharmacia LKB Biotechnology, Alameda, CA) to appropriate buffers. The dextran was mixed either in RB or the relaxing backup solution to 20% or 25% and solubilized by sonication. Dilution with the same buffer was used during experiments for lower concentrations.

Mechanical measurements

The tension produced by single muscle fibers was measured using either an Ackers 801 (Aksjelskapet, Norway) or a Cambridge 400A (Cambridge Technology, Watertown, MA) force transducer. The diameter was taken at three equally spaced points along the length of the fiber, at a magnification of 100× with a Nikon 2B (Nikon, Melville, NY) dissecting microscope. Fibers in backup and normal solutions (Table 1) did not differ in tension or stiffness. To ensure that the obtained results were not due to fiber deterioration in dextran solutions, tension was measured both before and after dextran experiments.

Muscle stiffness was measured using a length driver (model 6350; Cambridge Technology) and the Cambridge 400A force transducer, inter-

TABLE 1 Composition of the solutions used

Solutions	KAc (mM)	KPr (mM)	MOPS (mM)	$MgCl_2$ (mM)	EGTA (mM)	MgATP (mM)	$CaCl_2$ (mM)	NaN_3 (mM)	CP (mM)	CPK (units/ml)	Triton (%)	Glycerol (%)
FGB		130	20	2	1			1			0.5	25
FSB		130	20	2	1			1				50
RB (KAc)	60		20	5	1			1				
RB (KPr)		130	20	2	1			1				
Contraction		130	20	2	1	5	1.5	1				
Relaxation		130	20	2	1	5		1				
Low μ relaxation			20	2	1	5		1				
Contraction in backup			40	2	1	5	1.5	1	40	750		
Relaxation in backup			40	2	1	5		1	40	750		

All solutions were adjusted to pH 7.0 at 23°C.

faced to a personal computer via D/A board (DT2831G; Data Translation, Seattle, WA) and a function-generator board (SM1010; Signametrics, Seattle, WA). The instrument was controlled by a software program (DAC) developed at the University of Washington by the MCCM Programming Project. For each measurement, the fiber length was changed in steps of, 0.5, 0.7, 0.9, 1.1, and 1.3% of total fiber length, and the change in force was recorded. Stiffness, given by the slope of force against length, was calculated from a least-squares fit of the data. As with tension, stiffness was measured both before and after exposure to dextran to ascertain reversibility of the changes. All mechanical experiments were carried out at 23°C.

EPR and ST-EPR spectroscopy

EPR and saturation-transfer EPR (ST-EPR) experiments were performed on a Bruker ECS-106 spectrometer (Bruker Instruments, Billerica, MA). MSL-labeled fiber bundle was tied with surgical silk thread at the two ends and held isometrically inside a 50-μl fused-silica capillary tube (Wilmad Glass Company, Buena, NJ). The fiber-containing capillary was then placed in EPR cavities either perpendicular (TE_{102}) or parallel (modified TM_{110}; Thomas and Cooke, 1980) to the static magnetic field. Solution flowed continuously over the fibers at a rate of ~0.2–0.5 ml/min. A creatine phosphokinase-aided ATP backup system (Table 1) was used for the contracting and relaxing solutions during EPR measurements. Conventional EPR spectra were obtained in the TM_{110} cavity at 10-mW microwave power and 2-G field modulation (H_m). ST-EPR spectra were obtained in the TE_{102} cavity at a microwave field strength of 0.25 G, an H_m of 5 G, and a modulation frequency of 50 kHz.

In the EPR spectrum of myofibrils, which represents isotropically oriented spins, the P_1 peak (Fig. 3) has a width of 4.62 Gauss, and the P_2 region (Fig. 3) is a featureless intensity below the baseline before the high field trough (data not shown). Any departure from isotropic orientational distribution results in either the appearance of peaks at different positions of the spectrum and the concomitant loss of P_1 intensity or, if more spins orient along the z axis parallel to the field, a decrease in the P_1 line width (with parallel increase in height) and the appearance of positive intensity at P_2. Thus the P_1 intensity is sensitive to both types of spin redistribution, whereas P_2 is indicative of ordering about the axis parallel to the field.

Effective rotational correlation times (τ_R) were calculated from ST-EPR line-height ratios (L''/L) by comparison with a model system: MSL-labeled hemoglobin tumbling in a medium of known viscosity (Fajer and Marsh, 1982).

RESULTS

Isometric tension and stiffness

To determine the effect of dextran compression on force, isometric tension was measured in labeled and unlabeled fibers at varying concentrations of dextran. The relative values of tension, normalized to tension in the absence of dextran, are shown in Fig. 1. The tension initially rose, by 9.5% at 5% dextran for unlabeled and by 13% at 8% dextran for labeled fibers. This rise of tension is caused by compression of the lattice to original spacing by low levels of dextran (Maughan and Godt, 1979; Matsubara et al., 1985). At higher osmotic pressures the tension decreased linearly, reaching zero at 20–22% dextran. A shift to higher dextran concentration was observed in the tension curve of labeled fibers with respect to the unlabeled fibers (Fig. 1). This effect was due to increased radial stiffness of the labeled fibers as determined by fiber-diameter measurements. The labeled fibers required an additional 3–4% dextran to reach the same diameter as unlabeled fibers (data not shown).

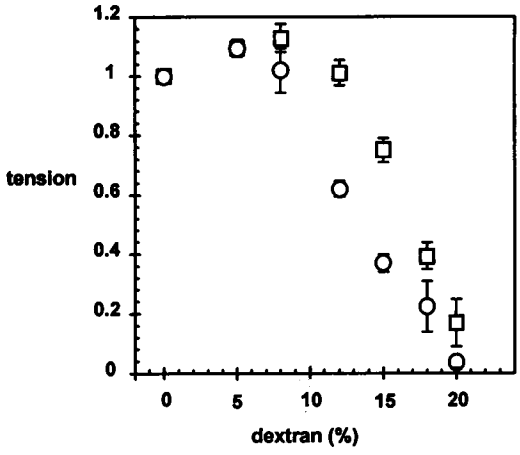

FIGURE 1 Isometric tension of labeled (□) and unlabeled (○) fibers as a function of dextran T-500 concentration. Each value is an average of at least five experiments, and the error bars represent ± SEM. Tension values are normalized to tension in the absence of dextran.

Because the decrease of tension can be due to decrease in either force generated per head or population of active heads, we have measured mechanical stiffness as an indicator of head attachment. Fig. 2 *A* shows axial stiffness of labeled fibers as a function of dextran in rigor, relaxation, and isometric contraction. Each value is normalized to that of rigor at 0% dextran. In rigor, stiffness increased by 13% for maximally compressed fibers. In relaxation, stiffness was constant up to 12% dextran, then increased rapidly from 0.05 to 0.4 at 20% dextran. The increase in stiffness beyond 12% dextran reflects steric constraints imposed by compressed lattice on myosin heads. In isometrically contracting fibers, three phases of concentration dependence can be delineated: between 0–5% dextran, stiffness remained constant; at 12% dextran, it increased by 0.2; and for maximally compressed fibers, stiffness decreased to 0.51. The difference in stiffness of 0.11 between relaxed and isometrically contracting conditions at 20% dextran suggests that the

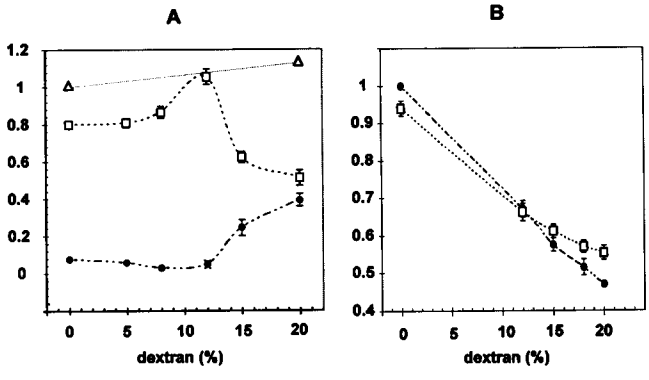

FIGURE 2 Stiffness (*A*) and diameter (*B*) of labeled fibers during rigor (*A*, △), contraction (□) and relaxation (●). Stiffness is normalized to that in rigor in the absence of dextran; diameter is normalized to diameter of relaxed fiber without dextran. Each value is an average of at least five experiments. The error bars represent ± SEM.

myosin heads are able to interact with actin even though no force is produced. To determine the levels of compression, we measured diameter of individual fibers in relaxed and isometric-contraction conditions (Fig. 2 *B*). In the absence of dextran, fiber diameter during relaxation was 6% more than during contraction. Compression resulted in a linear decrease of diameter in the relaxed fiber, whereas in contraction diameter changes strayed from linearity at higher compression levels, with smaller changes than for relaxed fiber. The cross-over point between these lines was at 12% dextran (Fig. 2 *B*), coinciding with the changes in tension dependence (Fig. 1) and stiffness (Fig. 2 *A*).

Myosin head orientation

Conventional EPR spectra of fibers oriented parallel to the magnetic field contain information about the orientational distribution of spin probes (Thomas and Cooke, 1980). The comparison of spectra at 0% and 20% dextran in rigor, relaxed, and isometrically contracting conditions is shown in Fig. 3. No changes in the spectra were observed in the rigor condition at any level of compression (Fig. 3, *left column*). We also found that the rigor heads were able to reorient back to their original orientations when the lattice was compressed in the relaxed state and rigor was induced under high osmotic pressure. The rigor bond is therefore able to form in highly compressed fibers and is stiff enough to bear full osmotic pressure. This high radial stiffness of rigor heads complements the high axial component of stiffness (Fig. 2 *A*).

In contrast to rigor, the relaxed fibers showed a dramatic change in fully compressed fibers (Fig. 3, *middle column*). The width of the low field resonance (Γ) decreased from 5.38 to 4.60 Gauss, and the intensity of the high field line (P_2) increased slightly above the baseline. Both spectral changes are indicative of increased axial order of the probe (Fajer, 1994). These spectral changes were completely reversible—when compression was removed the spectrum returned to original lineshape.

For the isometrically contracting fibers, the spectrum without dextran was similar to the relaxed spectrum (Fig. 3, *last column*), as found before for fibers labeled with lower specificity (Fajer et al., 1990b). The large disorder of the myosin heads accompanied by high stiffness suggests a broad range of orientations exhibited by the attached myosin heads in isometric contraction. As in relaxation, spectral changes upon maximum compression indicate increased ordering of the heads. The average linewidth of the low-field peak was 5.56 Gauss in the absence of dextran and decreased to 4.65 Gauss at 20% dextran.

To quantify the changes in the spectral lineshape, we plotted the amplitude (after normalization of spectra to the same integrated intensity) of the low field peak, P_1, against dextran in Fig. 4. P_1 curves for both relaxed and contracting fibers display a parabolic dependence, with slightly lower values for contraction. The difference between relaxed and contracting fibers reflects a difference in the orientational contribution between the active and the detached heads. The orientational distribution under these conditions is different from the isotropic distribution, because the P_1 value obtained from myofibril spectrum, 0.0028 ± 0.0002, was higher than that for relaxed fibers, 0.0026 ± 0.0001, and contracting fibers, 0.0024 ± 0.0001.

Myosin head mobility

To study the dynamics of the myosin heads in fibers, ST-EPR spectra were obtained under rigor, relaxed, and isometrically contracting conditions at various dextran concentrations. All ST-EPR spectra were obtained with the field aligned perpendicular to the fiber axis so as to minimize orientational effects and maximize sensitivity to rotational motion (Barnett and Thomas, 1984).

In rigor myosin heads are rigid on the microsecond time scale, as evident from the large integrated intensity and high line-height ratio ($L''/L > 1$) of the ST-EPR line shapes in

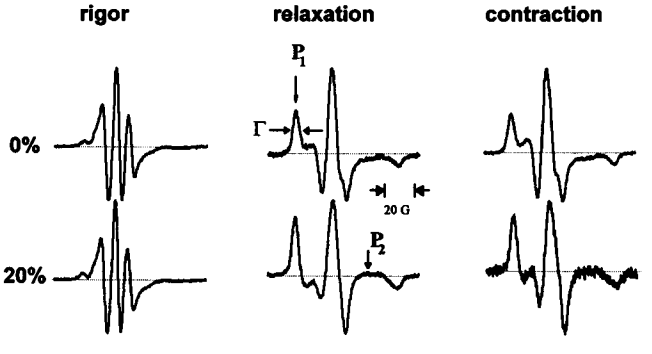

FIGURE 3 Conventional EPR spectra from fibers oriented parallel to the magnetic field. Columns from left to right: fibers in rigor, relaxed and isometrically contracting conditions at 0% (*upper row*) and 20% (*lower row*) dextran.

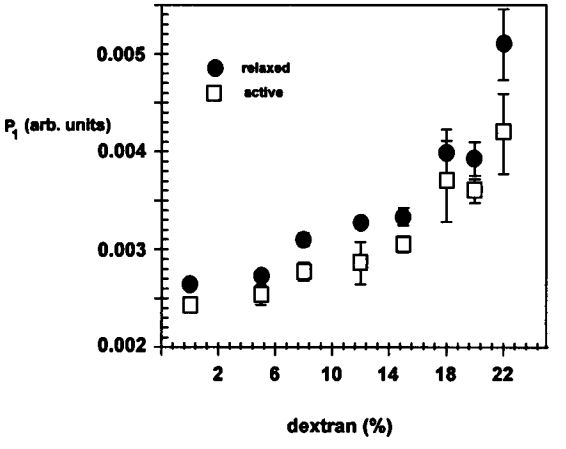

FIGURE 4 Low-field peak height (P_1) from conventional EPR spectrum in relaxed (●) and isometrically contracting (□) fibers in dextran. Spectra were normalized to the same integrated intensity.

Fig. 5. Osmotic compression did not affect the ST-EPR spectrum, implying that no motional changes were induced by dextran. Relaxed spectra in the absence of dextran are characteristic of species moving with an effective rotational correlation time, $\tau_R = 11 \pm 1$ μs, consistent with previous ST-EPR results (Thomas et al., 1980) and phosphorescence anisotropy decays (Stein et al., 1990). These motions are decreased in maximally compressed fibers: L''/L' increased from 0.53 to 0.83 and the integrated intensity increased by 60%, indicating motions with τ_R of 61 ± 9 μs. This decrease in mobility is partly due to the increase in viscous drag as implied by the increased stiffness in relaxation (Fig. 2 *A*).

The spectrum of contracting fibers in the absence of dextran indicates a mobility lower ($\tau_R = 30 \pm 2$ μs) than that of relaxed fibers. As in relaxation, 18% radial compression significantly inhibits microsecond mobility in contraction ($\tau_R = 231 \pm 15$ μs), resulting in a spectrum that is intermediate between those of rigor and relaxation (Fig. 5).

The changes in τ_R at increasing dextran concentrations is shown in Fig. 6. Compression initially resulted in a shallow, then, beyond 12–15% dextran, a sharply increasing τ_R for both relaxed and isometrically contracting fibers. In relaxed fibers τ_R changed linearly from 11 to 24 μs when compressed to 12% dextran but rose to 61 μs at 18% dextran. In the isometrically contracting fibers the initial increase of τ_R was more pronounced: from 30 μs in the absence of dextran, it increased to 83 μs at 12% dextran. Between 12% and 18% dextran, the decrease in mobility was even larger—τ_R increased by 148 μs.

The above effective correlation times, obtained by comparison to isotropically oriented samples, might be affected by the ordering of the heads observed in Fig. 4. This possibility is discounted, however, because the τ_R values obtained from fibers oriented perpendicular to magnetic field and from randomized myofibrils in relaxation were identical: at 0% dextran τ_R (myofibril) = 10 ± 3 μs compared to τ_R (fibers) = 11 ± 1 μs, and at 12% dextran τ_R (myofibril) = 25 ± 10 μs compared to τ_R (fibers) = 24 ± 3 μs. Thus, at least in the range of 0–12% dextran, the ordering of myosin heads does not affect estimates of their mobility. Above 12% dextran the ordering becomes more significant, as demonstrated by the sharp increase in P_1 in Fig. 4. This would result in higher L'' and lower L peak heights, increasing the L''/L ratio. Effective τ_R in this range may therefore be overestimated. In addition to the ordering effect, restriction of amplitude may also affect the ST-EPR spectra, but this effect is opposite the ordering effect: restricted amplitude of motion results in underestimation of effective τ_R (Howard et al., 1993). As ST-EPR is not capable of resolving amplitude and rate of motion, phosphorescence anisotropy decays (e.g., by Eads et al., 1984) would have to be employed to estimate the changes in amplitude of motion.

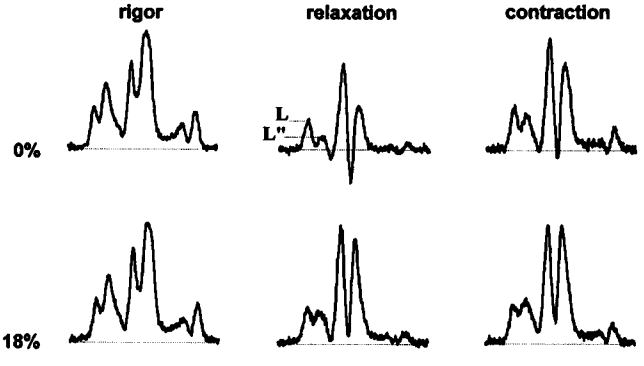

FIGURE 5 Gallery of saturation-transfer EPR spectra. Columns from left to right: spectra obtained from fibers in rigor, relaxation, and isometric contraction conditions at 0% (*upper row*) and 18% (*lower row*) dextran.

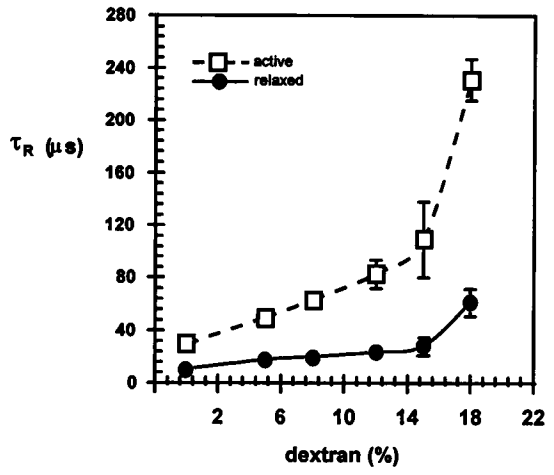

FIGURE 6 Effective correlation time (τ_R) for the isometrically contracting (□) and relaxed (●) fibers determined from low field ratio, L''/L, and hemoglobin calibration curve.

Notwithstanding the potential problems in the interpretation of effective correlation times at high compression, it is clear that the motion is significantly inhibited at compressions up to the critical spacing at 12% dextran. In relaxed fibers τ_R increased from 11 to 24 μs, whereas in contracting fibers τ_R increased from 30 μs in the absence of dextran to 83 μs at 12%. We find these changes significant because they did not result in the inhibition of muscle function.

DISCUSSION

The correlation of force generation and head dynamics revealed that the mobility of myosin heads in isometrically contracting fibers can be decreased by nearly threefold, from $\tau_R = 30$ μs to 83 μs, without any decrease in stiffness and tension. This finding implies that fast microsecond motions observed previously for the heads interacting with actin filaments are not coupled directly to force development. Furthermore, the inhibition of microsecond mobility is accompanied by the ordering of the myosin heads. Although no quantitative attempt was made to characterize the orientational disorder in the relaxed and active fibers, the ordering of the heads suggests that the active heads might be

more ordered then previously thought (Cooke et al., 1982; Fajer et al., 1990b).

Isometric tension and critical lattice spacing

Removal of the sarcolemma from muscle fibers is accompanied by swelling. Opposing radial forces, in the absence of sarcolemmal constraint, maintain equilibrium at a diameter slightly greater than that of intact fibers (Matsubara and Elliot, 1972; Maughan and Godt, 1979). These radial forces can be attributed to the electrostatic repulsion between the oppositely charged myofilaments and the elasticity originating from attached myosin heads as well as the fiber cytoskeletal structure (Irving and Millman, 1989; Brenner and Yu, 1991). Long-chain inert polymers, such as polyvinylpyrrolidone or dextran, can be used to provide osmotic compression on the swollen fibers, and once the original diameter is established, the fibers produce maximum tension (see, e.g., Godt and Maughan, 1977; Xu et al., 1993; Brenner and Yu, 1991). Compression below the intact diameter results in tension decline (Zhao and Kawai, 1993, and references cited therein).

In agreement with previous findings, the data presented here suggest that, at low concentrations of dextran (between 0 and 12%), there is a large decrease in fiber diameter (Fig. 2 *B*) but no decrease of tension (Fig. 1). When the diameter is reduced further, the tension declines sharply (Fig. 1), implying a minimum lattice spacing below which function is impaired. The labeled fibers display somewhat larger radial elasticity than the unlabeled fibers, but their general behavior under osmotic pressure is identical.

The critical diameter at 12% dextran, below which tension begins to decline (Fig. 2 *B*), coincides with the "equilibrium spacing" (the intersection of the two curves in Fig. 2 *B*), defined by Yu and co-workers as the diameter at which radial force produced by heads during the transition from relaxation to isometric contraction is zero (Brenner and Yu, 1991; Xu et al., 1993). As is evident in Fig. 2 *B*, the radial force generated by myosin heads during the transition from relaxation to isometric contraction is compressive above and expansive below the equilibrium spacing. At the equilibrium spacing, because the fiber diameter is compressed by 66%, the center-to-center spacing between the myosin and actin filaments is 18.7 nm (the average center-to-center spacing of relaxed fibers is 28.7 nm; Kawai et al., 1993), corresponding to an 8.2-nm available interfilament space for the myosin heads (assuming actin and myosin diameters are 8 and 13 nm, respectively), and is in agreement with the results of Gulati and co-workers, who also observed a sharp tension decline below a critical interfilament space of 6–9 nm (Gulati and Babu, 1982, 1985). The magnitude of this spacing is about half the long axis of myosin subfragment 1 (16.5 nm; Rayment et al., 1993), yet it does not inhibit myosin head function, as the tension is largely unaffected. An additional 2-nm decrease in diameter, however, corresponding to an interfilament space of 6.2 nm, results in complete inhibition of tension. Thus, for the myosin heads, a critical interfilament space of about 8.2 nm marks the minimum space necessary for full force generation.

Mobility and orientation versus force

MSL-labeled myosin heads in skinned fibers under rigor conditions are oriented at a single angle with a narrow angular distribution (Thomas and Cooke, 1980; Fajer, 1994). The orientation of the strongly attached heads in rigor is unperturbed by passive external forces along the fiber axis, as demonstrated previously by EPR (Cooke, 1981), by x-ray diffraction (Naylor and Podolsky, 1981), and by polarization of tryptophan fluorescence (dos Remedios et al., 1972). Whether negative axial strain has any effect on head angle is controversial (Burghardt and Ajtai, 1989; Fajer et al., 1991b). Complementing the axial perturbations, the present study shows that the rigor orientations are also not perturbed by radial strain (Fig. 3). At 20% dextran, the fiber diameter in rigor was decreased by about 78%, but the orientation of labeled domain remained constant.

EPR studies have shown that, in relaxation or during isometric contraction, the heads are dynamically disordered (Barnett and Thomas, 1989; Fajer et al., 1990b). The head disorder has also been confirmed by EM studies (Hirose et al., 1993) and by x-ray diffraction (Yu and Brenner, 1989). Unlike those in rigor, however, the head orientations in relaxation and isometric contraction are sensitive to compressive forces. Qualitatively, the changes in the line shapes are consistent with a decrease of the orientational disorder and tilting of the head toward the fiber axis. It is not hard to imagine that the detached heads under relaxation succumb to the decreasing lattice spacing by aligning along the fiber axis, which limits their orientational disorder. In isometric contraction the behavior of active heads in decreasing lattice spacing may not be as obvious, because the "rotating head" hypothesis predicts that the heads undergo large rotations while attached to the thin filaments. The changes were qualitatively similar under the two conditions, however. Rigorous analysis of the spectra by extensive computer simulations, currently under way, is expected to provide quantitative details, but despite the lack of detailed description, the present results establish that the heads must maintain a large disorder and a minimum average angle with respect to the fiber axis to generate maximum tension.

This study addresses the issue of myosin head motions in fibers directly associated with the force-generating transitions by correlating the mobility of the heads with their ability to generate force. In contrast to the fast motions of attached heads observed earlier in solution and fiber studies (Berger et al., 1989; Barnett and Thomas, 1989), this study shows that in isometrically contracting fibers the head motions can be inhibited threefold without a decrease in force. The faster motions observed in uncompressed fibers are thus an overestimate of the actual motions needed for force

generation. One can speculate that the fast motions observed previously in skinned fibers with swollen lattice or from proteins in solution arise from thermal fluctuations due to the expanded interfilament space. Furthermore, the dramatic difference in the motions between compressions below and above 12% dextran, corresponding to the equilibrium spacing, shows that inhibition of motions slower than τ_R = 80–90 μs is accompanied by the onset of tension inhibition. These results suggest that a minimum mobility corresponding to the critical lattice spacing is necessary for force generation.

Previous ST-EPR studies have shown that the heads in relaxation and isometric contraction are characterized by τ_R = 10 and 25 μs, respectively (Barnett and Thomas, 1989). Comparable but complex motions were obtained from time-resolved phosphorescence studies, which showed the head rotations consisting of distinct modes of motions with a τ_R of approximately 10 and 150 μs in relaxation and twice as slow in isometric contraction (Stein et al., 1990). Because the measured τ_R during isometric contraction represents an ensemble average of motions occurring within the various states of the steady-state hydrolysis cycle, not all of these motions may be directly coupled with force generation. The approach has been, therefore, to isolate distinct states of the hydrolysis cycle and to determine the myosin head mobility in each state independently. In particular, the attached states have been the focus of interest, as force is generated from a transition between two or more attached states.

In the weakly attached states, induced by relaxation at low-ionic-strength conditions (Fajer et al., 1991a) or in the presence of ATPγS and Ca^{2+} (Fajer et al., 1995), the heads undergo rotations nearly identical to those of the detached heads in relaxation. Similar findings of fast motions of weakly attached heads in ATPγS was also reported in myofibrils (Berger and Thomas, 1993, 1994). Compared to these fast motions in the weakly attached states, the mobility of the heads in the strongly attached states was found to be much slower. In the putative pre-power-stroke state trapped by aluminum fluoride, the fast motions were inhibited: $\tau_R \sim$ 150 μs (Raucher and Fajer, 1994). After force generation, the states trapped by ADP, AMPPNP, and PP_i show the heads to be as rigid as rigor: $\tau_R >$ 1 ms (Raucher et al., 1994; Fajer et al., 1988; Berger and Thomas, 1994). In all of the above studies, excluding the myofibril experiments where orientational study was not feasible, the orientation of myosin heads in the weakly attached states and the pre-power-stroke state was disordered, as in relaxation, whereas in the strongly attached post-power states, it was mostly ordered at a well-defined angle (references as above; Pate and Cooke, 1988; Fajer et al., 1990a; Zhao et al., 1995a,b).

Taken together, these studies indicate the following probable sequence of events: the weakly attached states early in the hydrolysis cycle are disordered and mobile on the microsecond time scale (τ_R = 2–10 μs); the heads then attach strongly decreasing their mobility, but not steriospecifically (maintaining orientational disorder). The force generation involves a *disorder-to-order transition* of the strongly attached heads, leads the cycle to its end, where the heads are strongly attached, rigid, and oriented (Raucher and Fajer, 1994). Although plausible, this sequence of events lacked a direct correlation with function. The results presented here demonstrate a limited disorder and mobility necessary for maintaining tension, indicating that both the disorder of the heads and their mobility now have clear functional implications, and they reinforce and extend earlier ideas (Raucher and Fajer, 1994; Raucher et al., 1995; Thomas et al., 1995) that force is generated in the strongly attached states due to a *disorder-to-order transition* of the myosin heads characterized by intermediate mobility.

Modeling of attached head mobility

Under conditions of slow exchange, one can deconvolute the composite ST-EPR spectrum obtained during contraction into spectra arising from attached and detached populations of myosin heads. In terms of the line-height ratio, L''/L, mobility of the attached heads can be obtained from

$$(L''/L)_{\text{attached}} = [L''_{\text{contraction}} - (1-f) * L''_{\text{relaxation}}]/(f * L), \quad (1)$$

where f is the attached fraction, L is the average of $L_{\text{contraction}}$ and $L_{\text{relaxation}}$ at each concentration of dextran ($L_{\text{contraction}} \approx L_{\text{relaxation}}$, within experimental error), and relaxed spectrum is assumed identical to the detached spectrum.

Fig. 7 shows the mobility of attached heads as a function of dextran concentration when f is taken as the difference between stiffness of contraction and relaxation (corrected for the same diameter). At 0% dextran, the mobility of attached heads is much lower (τ_R = 44 μs) than that of all heads (τ_R = 30 μs). Below the equilibrium spacing (12% dextran), the mobility of attached heads decreases from 44 to 91 μs, most of this decrease accompanying the compression of the swollen lattice to optimum spacing at 8% dextran. Beyond 12% dextran a dramatic decrease in the mo-

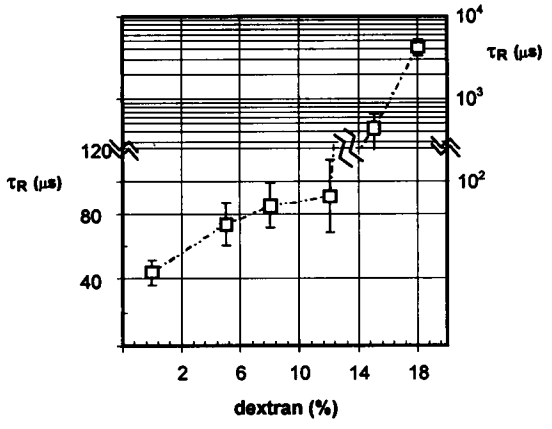

FIGURE 7 τ_R of attached myosin heads in isometric contraction in dextran. The fraction of attached heads, determined from stiffness, was used to calculate τ_R from the peak height ratios at each concentration of dextran (see text for details).

bility, parallel with the decrease of tension, is observed. If, instead of a double-headed cross-bridge, a single-headed attachment is assumed (Fajer et al., 1988; Pate and Cooke, 1988), then the fraction of attached heads = $f/2$, and the mobility is even lower: τ_R = 180 μs at 0% dextran, 360 μs at 8–12% dextran, and in the millisecond region beyond 12% dextran.

Both scenarios above assumed that all sarcomere compliance originates from cross-bridges. However, recent studies suggest that as much as 50% compliance may originate from the thick and thin filaments (Huxley et al., 1994; Wakabayashi et al., 1994; Huxley, 1995; Higuchi et al., 1995). In that case, the number of attached heads (n) is a nonlinear function of stiffness [$n(x) = 0.5x/(0.5 + x)$, where x is the measured stiffness]. The resulting mobility of attached heads during contraction is then τ_R = 337 μs at 0% dextran, 1110 μs at 12% dextran, and 6.5 ms and 60 ms at 15% and 18% dextran, respectively. Although the absolute values of τ_R change according to the different models of stiffness, all models indicate about a two- to threefold decrease of mobility between 0 and 12% dextran followed by a sharp inhibition of mobility at higher dextran concentrations.

So far we have made no distinction between the weakly attached and strongly attached heads. In principle, the observed decrease in mobility could be due to the weakly attached heads alone. To account for this possibility we measured the mobility of the weakly attached heads relaxed at the low ionic strength and low (5°C) temperature. In the absence of compression, the mobility of these heads was 30 ± 5 μs. Compression by 12% dextran decreased the mobility to 45 ± 10 μs. Contribution of the weakly attached heads to the overall mobility in the isometric contraction at 12% dextran can be estimated, assuming that at most 25% of heads are detached or weakly attached (Zhao and Kawai, 1993). The mobility of strongly attached heads would then be τ_R = 96 μs [(83 μs − 0.25 * 45 μs)/0.75].

Independent from the assumed scenario, the mobility of attached heads during contraction is less than 80 μs. This mobility is significantly lower than the previous estimates. Although we cannot distinguish between the strongly attached force-generating heads and the strongly attached non-force-producing heads, it seems unlikely that the force-producing heads would have lower mobility than the heads immediately before force generation ($\tau_R \gg$ 80 μs) and immediately after force generation (in rigor τ_R = 2–3 ms, and in ADP τ_R = 1800–2800 μs; Raucher and Fajer, 1994). More likely, the head undergoes a series of conformational changes in which the overall mobility is progressively inhibited, corresponding to more stereospecific and biochemically stronger actomyosin complexes. In the latter case, 80-μs motions would be the upper bound for the mobility associated with force generation. Inhibition of faster motions does not correlate with loss of tension, whereas the damping of these 80-μs motions leads to loss of tension, as observed here.

We would like to thank April Dail and Anne Thistle for editorial help and Steve Mnookin for initial tension experiments.

This research was sponsored by the National Science Foundation (IBN-953064), and by the American Heart Association (GIA-9501335), and a student grant from the American Heart Association (BA).

REFERENCES

Barnett, V. A., and D. D. Thomas. 1984. Saturation transfer electron paramagnetic resonance of spin-labeled muscle fibers: dependence on sarcomere length. *J. Mol. Biol.* 179:83–102.

Barnett, V. A., and D. D. Thomas. 1989. Microsecond rotational motion of spin-labeled myosin heads during isometric muscle contraction. *Biophys. J.* 56:517–523.

Berger, C. L., E. C. Svensson, and D. D. Thomas. 1989. Photolysis of a photolabile precursor of ATP (caged ATP) induces microsecond rotational motions of myosin heads bound to actin. *Proc. Natl. Acad. Sci. USA.* 86:8753–8757.

Berger, C. L., and D. D. Thomas. 1991. Rotational dynamics of actin-bound intermediates in the myosin ATPase cycle. *Biochemistry.* 30: 11036–11045.

Berger, C. L., and D. D. Thomas. 1993. Rotational dynamics of actin-bound myosin heads in active myofibrils. *Biochemistry.* 32:3812–3821.

Berger, C. L., and D. D. Thomas. 1994. Rotational dynamics of actin-bound intermediates of the myosin adenosine triphosphatase cycle in myofibrils. *Biophys. J.* 67:250–261.

Brenner, B., and L. C. Yu. 1991. Characterization of radial force and radial stiffness in Ca^{2+}-activated skinned fibres to the rabbit psoas muscle. *J. Physiol. (Lond.).* 441:703–717.

Burghardt, T. P., and K. Ajtai. 1989. Effect of negative mechanical stress on the orientation of myosin cross-bridges in muscle fibers. *Proc. Natl. Acad. Sci. USA.* 86:5366–5370.

Cooke, R. 1981. Stress does not alter the conformation of a domain of the myosin cross-bridge in rigor muscle fibres. *Nature.* 194:570–571.

Cooke, R., M. S. Crowder, and D. D. Thomas. 1982. Orientation of spin labels attached to cross-bridges in contracting muscle fibres. *Lett. Nature.* 300:776–778.

Crowder, M. S., and R. Cooke. 1984. The effect of myosin sulphydryl modification on the mechanics of fiber contraction. *J. Muscle Res. Cell. Motil.* 5:131–146.

dos Remedios, C. G., R. G. C. Millikan, and M. G. Morales. 1972. Polarization of tryptophan fluorescence from single striated muscle fibers. *J. Gen. Physiol.* 59:103–120.

Eads, T. M., D. D. Thomas, and R. H. Austin. 1984. Microsecond rotational motions of eosin-labeled myosin measured by time-resolved anisotropy of absorption and phosphorescence. *J. Mol. Biol.* 179:55–81.

Eisenberg, E., and T. L. Hill. 1985. Muscle contraction and free energy transduction in biological systems. *Science.* 227:999–1006.

Fajer, P. G. 1994. Method for the determination of myosin head orientation from EPR spectra. *Biophys. J.* 66:2039–2050.

Fajer, P. G., E. A. Fajer, H. J. Brunsvold, and D. D. Thomas. 1988. Effects of AMPPNP on the orientation and rotational dynamics of spin-labeled myosin heads in muscle fibers. *Biophys. J.* 53:513–524.

Fajer, P. G., E. A. Fajer, J. J. Matta, and D. D. Thomas. 1990a. Effect of ADP on the orientation of spin-labeled myosin heads in muscle fibers: a high-resolution study with deuterated spin labels. *Biochemistry.* 29: 5865–5871.

Fajer, P. G., E. A. Fajer, M. Schoenberg, and D. D. Thomas. 1991a. Orientational disorder and motion of weakly attached cross-bridges. *Biophys. J.* 60:642–649.

Fajer, P. G., E. A. Fajer, and D. D. Thomas. 1990b. Myosin heads have a broad orientational distribution during isometric muscle contraction: time-resolved EPR studies using caged ATP. *Proc. Natl. Acad. Sci. USA.* 87:5538–5542.

Fajer, P. G., P. Johnson, and D. D. Thomas. 1991b. Myosin head orientation in negatively strained cross-bridges. An EPR study. *Biophys. J.* 59:419a.

Fajer, P., and D. Marsh. 1982. Microwave and modulation field inhomogeneities and the effect of cavity Q in saturation transfer ESR spectra. Dependence on sample size. *J. Magn. Res.* 49:212–224.

Fajer, E. A., E. M. Ostap, D. D. Thomas, N. Naber, and P. G. Fajer. 1995. Orientation and dynamics of myosin heads in ATPγS and Ca^{2+}. *Biophys. J.* 68:322s.

Godt, R. E., and D. W. Maughan. 1977. Swelling of skinned muscle fibers of the frog. *Biophys. J.* 19:103–116.

Gulati, J., and A. Babu. 1982. Tonicity effects on intact single muscle fibers: relation between force and cell volume. *Science.* 215:1109–1112.

Gulati, J., and A. Babu. 1985. Critical dependence of calcium-activated force on width in highly compressed skinned fibers of the frog. *Biophys. J.* 48:781–787.

Harada, Y., A. Noguchi, A. Kishino, and T. Yanagida. 1987. Sliding movement of single actin filaments on one headed myosin filaments. *Nature.* 326:605–608.

Harada, Y., K. Sakurada, T. Aoki, D. D. Thomas, and T. Yanagida. 1990. Mechanochemical coupling in actomyosin energy transduction studied by in vitro movement assay. *J. Mol. Biol.* 216:49–68.

Higuchi, H., T. Yanagida, and Y. E. Goldman. 1995. Compliance of thin filaments in skinned fibers of rabbit skeletal muscle. *Biophys. J.* 69: 1000–1010.

Hirose, K., T. D. Lenart, J. M. Murray, C. Franzini-Armstrong, and Y. E. Goldman. 1993. Flash and smash: rapid freezing of muscle fibers activated by photolysis of caged ATP. *Biophys. J.* 65:397–408.

Howard, E. C., K. M. Lindahl, C. F. Polnaszek, and D. D. Thomas. 1993. Simulation of saturation transfer electron paramagnetic resonance spectra for rotational motion with restricted angular amplitude. *Biophys. J.* 64:581–593.

Huxley, A. F., and R. M. Simmons. 1971. Proposed mechanism of force generation in striated muscle. *Nature.* 233:533–538.

Huxley, H. E. 1969. The mechanism of muscular contraction. *Science.* 164:1356–1366.

Huxley, H. E. 1995. The working stroke of myosin cross-bridges. *Biophys. J.* 55s–58s.

Huxley, H. E., A. Stewart, H. Sosa, and T. Irving. 1994. X-ray diffraction measurements of the extensibility of actin and myosin filaments in contracting muscle. *Biophys. J.* 67:2411–2421.

Irving, T., and B. M. Millman. 1989. Changes in thick filament structure during compression of the filament lattice in relaxed frog sartorius muscle. *J. Muscle Res. Cell Motil.* 10:385–396.

Kawai, M., J. S. Wray, and Y. Zhao. 1993. The effect of lattice spacing change on cross-bridge kinetics in chemically skinned rabbit psoas muscle fibers. Proportionality between the lattice spacing and the fiber width. *Biophys. J.* 64:187–196.

Lymn, R. W., and E. W. Taylor. 1971. Mechanism of adenosine triphosphate hydrolysis by actomyosin. *Biochemistry.* 10:4617–4624.

Matsubara, I., and G. F. Elliot. 1972. X-ray diffraction studies on skinned single fibers of frog skeletal muscle. *J. Mol. Biol.* 72:657–669.

Matsubara, I., Y. Umazume, and N. Yagi. 1985. Lateral filamentary spacing in chemically skinned murine muscles during contraction. *J. Physiol. (Lond.).* 360:135–184.

Maughan, D. W., and R. E. Godt. 1979. Stretch and radial compressed studies on relaxed skinned muscle fibers of the frog. *Biophys. J.* 28: 391–402.

Naylor, G. R., and R. J. Podolsky. 1981. X-ray diffraction of strained muscle fibers in rigor. *Proc. Natl. Acad. Sci. USA.* 78:5559–5563.

Pate, E., and R. Cooke. 1988. Energetics of the actomyosin bond in the filament array of muscle fibers. *Biophys. J.* 53:561–573.

Raucher, D., and P. G. Fajer. 1994. Orientation and dynamics of myosin heads in aluminium fluoride induced pre-power stroke states—an EPR study. *Biochemistry.* 33:11993–11999.

Raucher, D., C. P. Sar, K. Hideg, and P. G. Fajer. 1994. Myosin catalytic domain flexibility in MgADP. *Biochemistry.* 33:14317–14323.

Raucher, D., E. A. Fajer, C. Sar, K. Hideg, Y. Zhao, M. Kawai, and P. G. Fajer. 1995. A novel electron paramagnet resonance spin label and its application to study the cross-bridge cycle. *Biophys. J.* 68:128s–133s.

Rayment, I., W. R. Rypniewski, K. Schmidt-Base, R. Smith, D. R. Tomchick, M. M. Benning, D. A. Winkelman, G. Wesenberg, and H. M. Holden. 1993. The three-dimensional structure of a molecular motor, myosin subfragment-1. *Science.* 261:50–58.

Stein, R. A., R. D. Ludescher, P. S. Dahlberg, P. G. Fajer, R. L. H. Bennett, and D. D. Thomas. 1990. Time-resolved rotaional dynamics of phosphorescent-labeled myosin heads in contracting muscle fibers. *Biochemistry.* 29:10023–10031.

Thomas, D. D., and R. Cooke. 1980. Orientation of spin-labeled myosin heads in glycerinated muscle fibers. *Biophys. J.* 32:891–906.

Thomas, D. D., S. Ishiwata, J. C. Seidel, and J. Gergely. 1980. Submillisecond rotational dynamics of spin-labeled myosin heads in myofibrils. *Biophys. J.* 32:873–890.

Thomas, D. D., S. Ramachandran, O. Roopnarine, D. W. Hayden, and E. M. Ostap. 1995. The mechanism of force generation in myosin: a disorder-to-order transition, coupled to internal structural changes. *Biophys. J.* 68:135s–141s.

Wakabayashi, K., Y. Sugimoto, H. Tanaka, Y. Ueno, Y. Takezawa, and Y. Amemiya. 1994. X-ray diffraction evidence for the extensibility of actin and myosin filaments during muscle contraction. *Biophys. J.* 67: 2422–2435.

Xu, S., B. Brenner, and L. C. Yu. 1993. State-dependent radial elasticity of attached cross-bridges in single skinned fibres of rabbit psoas muscle. *J. Physiol.* 461:283–299.

Yanagida, T., T. Arata, and F. Oosawa. 1985. Sliding distance of actin filament induced by a myosin crossbridge during one ATP hydrolysis cycle. *Nature.* 316:366–369.

Yu, L. C., and B. Brenner. 1989. Structures of actomyosin cross-bridges in relaxed and rigor muscle fibers. *Biophys. J.* 55:441–453.

Zhao, L., N. Naber, and R. Cooke. 1995a. Muscle cross-bridges bound to actin are disordered in the presence of 2,3-butanedione monoxome. *Biophys. J.* 68:1980–1990.

Zhao, L., E. Pate, A. Bohen, and R. Cooke. 1995b. The myosin catalytic domain does not rotate during the power stroke. *Biophys. J.* 68:362s.

Zhao, Y., and M. Kawai. 1993. The effect of the lattice spacing change on cross-bridge kinetics in chemically skinned rabbit psoas muscle fibers. II. Elementary steps affected by the spacing change. *Biophys. J.* 64: 197–210.